COO-4246-3

MICROSTRUCTURAL EFFECTS IN ABRASIVE WEAR

Quarterly Progress Report
for the period 15 September - 15 December 1977

Nicholas F. Fiore
Department of Metallurgical Engineering and Materials Science
Notre Dame, IN 46556

NOTICE
This report was prepared as an account of work sponsored by the United States Government. Neither the United States nor the United States Department of Energy, nor any of their employees, nor any of their contractors, subcontractors, or their employees, makes any warranty, express or implied, or assumes any legal liability or responsibility for the accuracy, completeness or usefulness of any information, apparatus, product or process disclosed, or represents that its use would not infringe privately owned rights.

1 January 1978

Prepared for

U. S. Department of Energy

Under Contract No. EF-77-S-02-4246

DISCLAIMER

CONTENTS

ABSTRACT

A series of alloy white irons and Co-base superalloys are being tested for low-stress abrasion resistance in a rubber-wheel abrasion test (RWAT) and for gouging wear resistance in a grinding wheel test (GWAT). The objective of the tests is to establish general relations for the improvement of wear resistance by the control of microstructure.

Wear testing on the white irons has been completed. The test results indicate that microstructural factors such as carbide shape, volume fraction and the presence of retained austenite greatly influence wear resistance. Macrohardness provides a good measure of low-stress wear resistance, but is less effective as a measure of gouging wear resistance. In cases of uniform matrices, matrix microhardness, rather than carbide microhardness, correlates with both low-stress and gouging wear resistance.

For Ni-Hard 4 white iron, RWAT and GAWT wear resistance can be correlated with mechanical properties obtained in compression, fatigue, impact and fracture toughness tests. The most direct correlations are obtained for hardness and compression tests.

Work is now underway to quantify the wear-microstructure relations and to develop an understanding of the relationship between wear, microstructure and mechanical properties.

1. OBJECTIVE AND SCOPE

The objective of this research program is to establish quantitative relations between microstructure and abrasive wear resistance under gouging and low-stress conditions. The materials to be studied include low-to-high Cr white irons and Co-base powder metallurgy alloys commonly used for abrasion resistance in coal mining, handling and gasification. The two-year contract was initiated on 15 March, 1977, and during this third quarter of the first year progress has been in the following areas:

1. Gouging abrasive wear tests (GAWT) have been completed on white irons of various alloy content and on a series of Ni-hard 4 irons containing 5 to 85% retained austenite (γ). The microstructural effects revealed in the GAW tests have been compared with rubber wheel abrasive (RWAT) test results on the same two sets of materials.

2. Metallography has been completed on the Ni-hard 4 series.

3. A survey of the use of quantitative microscopy (QTM) techniques to characterize microstructure of the alloys employed in the program has been completed.

4. The mechanical properties of the white irons and Ni-hard 4 series have been obtained and tabulated. The properties which correlate to GAWT and RWAT wear resistance have been identified.

5. A series of generalizations relating mechanical properties, microstructure and wear resistance of cast irons have evolved, and these may present guidelines in materials' selection and alloy design.

Each of these areas of progress lies within the five Tasks specified in the contract. They are discussed in more detail in the following section, "TASKS AND PROGRESS".

2. TASKS AND PROGRESS

2.1 Task I - Preparation of Test Matrix

This task is complete. The matrix was prepared and forwarded to ERDA - Chicago Operations Office on 6 June 1977. It is described in the contract quarterly report COO-4246-1.

2.2 Task II - Preparation of Materials

This task is now accomplished. The contract specifies testing of wear-reistant white irons and Co-base powder metallurgy alloys. The materials to be tested are listed in Tables I and II. All of these materials have now been procured and cut to appropriate specimen size. The alloy irons (items 2,3,4 of Table I) have been supplied by Climax Molybdenum Corporation in the form of cast plates 190 mm x 137 mm x 21 mm. The Ni-hard 4 samples (item 1 of Table I), also supplied by Climax, are in the form of compact-tension fracture toughness specimens 60 mm x 56 x 13 mm. The Co-base powder metallurgy alloys obtained from Stellite Division, Cabot Corporation, are in the form of pressed and sintered plates 50 mm x 25 mm x 13 mm.

2.3 Task III - Wear Testing

2.3.1 General Features of the RWAT and GAWT

The detailed procedures for the RWAT and the GAWT measurements have been presented in quarterly report COO-4246-2. In the RWAT, a quartz sand is abraded across the specimen surface by means of a rotating rubber wheel. The wheel travels 713 m during the course of a test. In the GAWT, an Al_2O_3 grinding wheel is rotated across the sample, traveling 732 m during the course of the test. Thus the total distance traveled by abrasive is essentially identical in the two tests, so specimen weight losses may be directly compared. The RWAT wear data are reported directly as specimen weight loss per test (i.e. specimen weight loss/713 m of abrasive travel). The GAWT data are reported as AF, the Abrasion Factor (specimen weight loss per 732 m/1020 steel weight loss per 732 m). Under the test conditions, the 1020 steel weight loss is normally about 1.0 g; thus the AF of the specimen is very close to its weight loss per 732 m. For these reasons both the RWAT and GAWT data may be thought of as representing specimen weight loss per about 720 m of abrasive travel under the two respective test conditions.

Both the RWAT and the GAWT have proven to be highly reproducible, having coefficients of variation v of the order of 2 to 4 percent. (Statistical analysis applied to wear testing is discussed in detail elsewhere [1,2,3]). Each wear datum point presented represents the mean of at least 3 individual tests. Means outside of $\pm$ 3 σ control limits are disregarded, and the three tests repeated. Thus far in the entire test program, data have fallen outside of the control limits on only two occasions, once in the case of RWAT test series and once in the case of a GAWT test series.

Table I. Wear-Resistant Irons

Type	Microstructural Condition
1. ASTM532 - Type I - Ni-Hard 4	Cr_7Cr_3 Carbides in Tempered Martensite with a. 5% Retained Austenite b. 20% " " c. 40% " " d. 85% " "
2. ASTM532 - Type II - (15 Cr-3 Mo)	Cr_7C_3 Carbides in Tempered Martensite (overtempered)
3. ASTM532 - Type III- (27 Cr-2.5C)	Cr_7C_3 Carbides in Tempered Martensite
4. Pearlitic White Iron	Fe_3C Carbides in Pearlitic Matrix a. 3.5C - High Carbide Vol. Frac. b. 2.7C - Low Carbide Vol. Frac.

Table II. Co-base Powder Metallurgy Alloys

Type		Microstructure
1. #6	Low carbide vol. frac.	Low solid solution strengthener content.
2. #6KC-L	Moderate carbide vol. fraction	Low solid solution strengthener content.
3. #6KC-H	High carbide vol. frac.	Low solid solution strengthener content.
4. #19	High carbide vol. frac.	Moderate solid solution strengthener content.
5. #98M2	High carbide vol. frac.	High solid solution strengthener content.
6. #3	Very high carbide vol. fraction	High solid solution strengthener content.
7. #Star-J	Very high carbide vol. fraction	Very high solid solution strengthener content.

2.3.2 RWAT and GAWT Results on White Irons

Figures 1 and 2 consist of RWAT and GAWT histograms for 2.7C and 3.5C pearlitic white irons, 15 Cr - 3 Mo and 27 Cr irons. The RWAT data have been obtained for wear directions both normal to and cross the solidification direction. The GAWT data have been obtained for the normal, cross and parallel directions. The microstructures of the irons are shown in Figures 3 and 4. These have been discussed in the previous quarterly report COO 4246-2 and are included here for the sake of completeness.

A number of generalizations are evident from Figures 1 and 2.

1. For all materials, the GAWT, with its rigidly supported Al_2O_3 abrasive of high hardness (Knoop Hardness Number KHN = 1650), produces about 10 times the weight loss of the RWAT, in which the softer SiO_2 abrasive (KHN 750) relaxes into the rubber tire. This is expected since the GAWT has been developed to simulate gouging wear, which is more a traumatic process than low-stress abrasive wear.

2. For the two low-alloy peralitic irons, both RWAT and GAWT wear resistance increases as C content (Fe_3C volume fraction) increases. This is consistent with the usual interpretation that Fe_3C is responsible for imparting wear resistance to pearlitic white irons.

3. For the two low-alloy pearlitic white irons, RWAT and GAWT wear resistance is greater across dendrites than normal to dendrites. In the GAWT results, maximum wear resistance is obtained parallel to dendrite long axes. These data indicate clearly that phase shape may be exploited in optimizing wear resistance.

4. Considering its relatively high alloy content, the 15 Cr - 3 Mo alloy has mediocre RWAT and GAWT wear resistance. Its hard and highly alloyed Cr_7C_3 carbides are supported in a soft matrix of overtempered martensite. This indicates that carbide hardness must be coupled with appropriate matrix properties to justify the expense of alloying to increase wear resistance.

5. The RWAT and GAWT wear resistance of the 27 Cr iron are greatest. This highly alloyed iron consists of needle-like Cr_7C_3 carbides more or less randomly arranged in a hard matrix of lightly tempered martensite. Its excellent wear resistance is expected in view of its overall hardness. The lack of orientation dependence of wear resistance is not surprising since the carbides in the alloy are not aligned preferentially relative to the solidification front.

2.3.3 RWAT and GAWT Testing of Ni-Hard 4.

The microstructures of the Ni-Hard 4 samples are given in Figures 5 through 8. The structures were produced from a single heat of the alloys processed so as to generate four amounts of retained austenite. (See Table I). In general they consist of massive white carbides in a matrix of tempered martensite and retained γ. The martensite tends to appear needle-like and dark-etching at high magnifications, although the amount present is not determinable by QTM techniques. Instead the percentages of retained γ have been established at 5, 20, 40 and 85% in X-ray studies conducted at the Climax Molybdenum research laboratories.

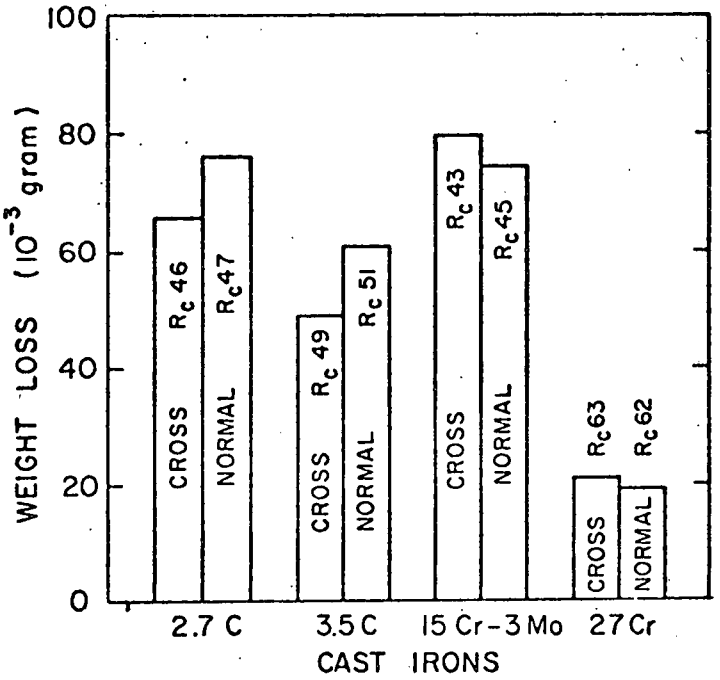

Figure 1. A comparison of RWAT weight loss for four white cast irons, each tested in two orientations relative to the solidification front.

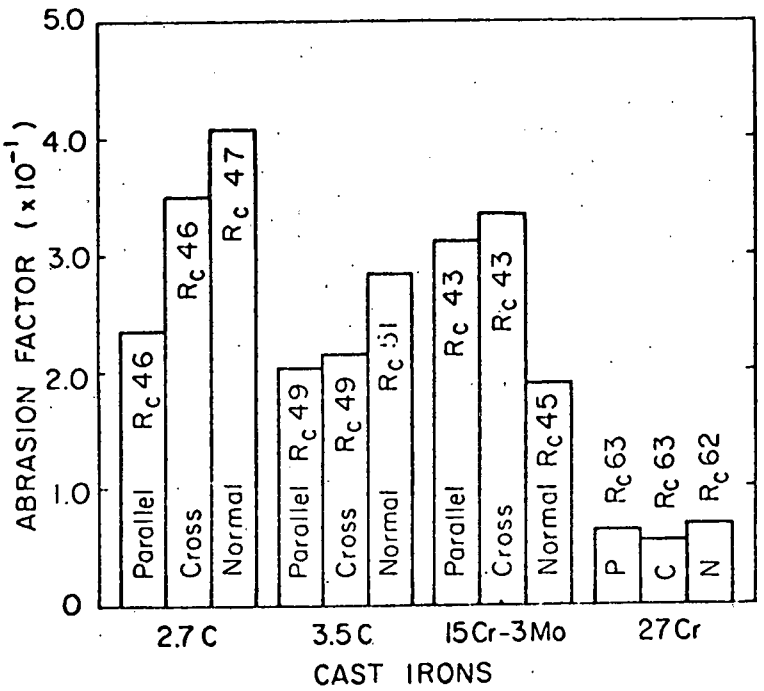

Figure 2. A comparison of GAWT abrasion factor for four white cast irons, each tested in three orientations relative to the solidification front.

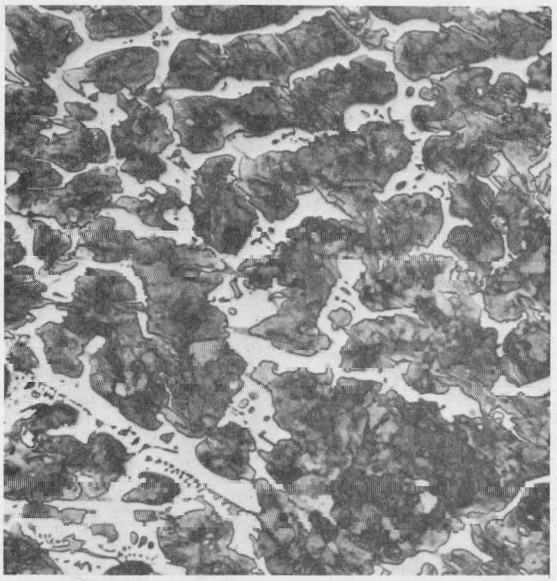

2.7C Cross

2.7C Normal

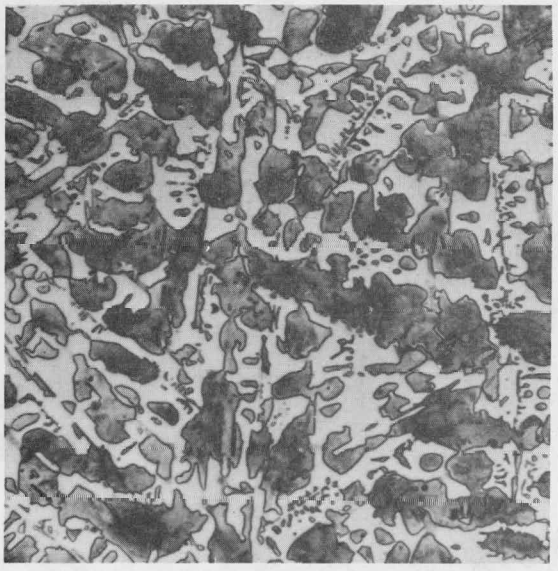

3.5C Cross

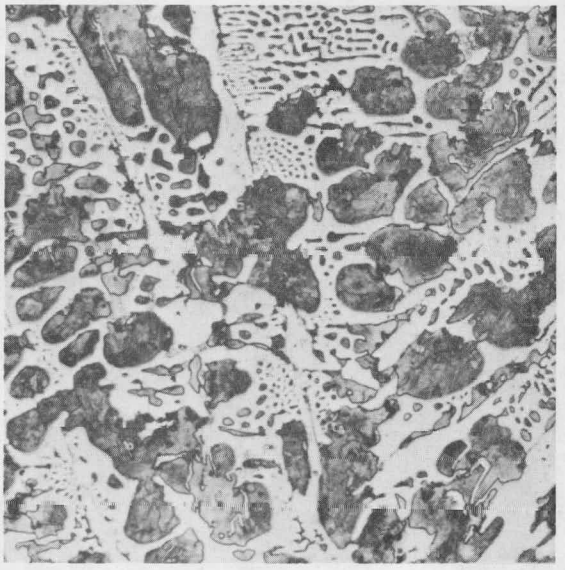

3.5C Normal

Fig.3. Microstructures of a "high" and a "low" carbon pearlitic white cast iron showing the difference in amount of eutectic carbide and the variation of structure with solidification direction. 100X.

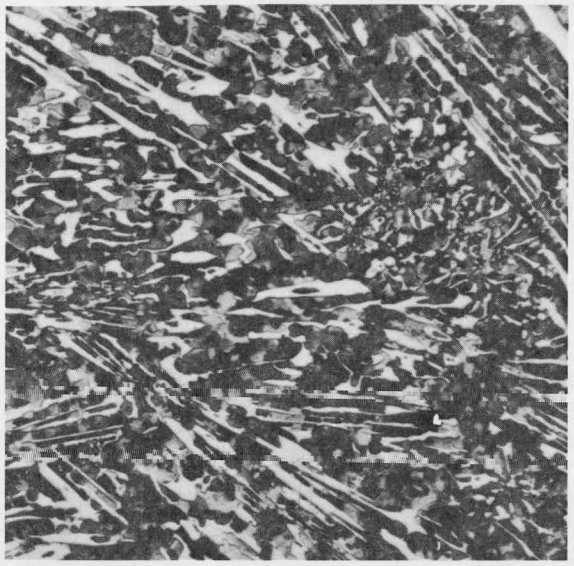

a) 15Cr-3Mo Cross

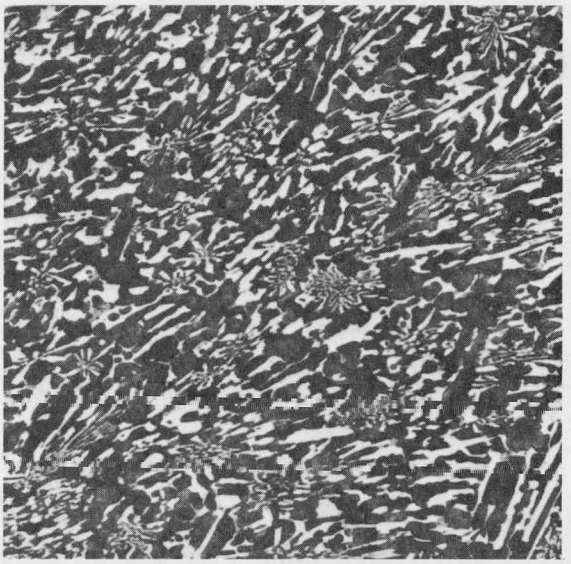

b) 15Cr-3Mo Normal

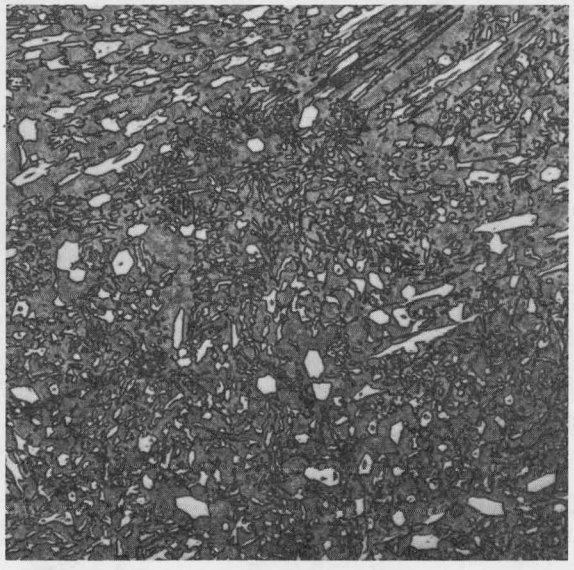

c) 27Cr Cross

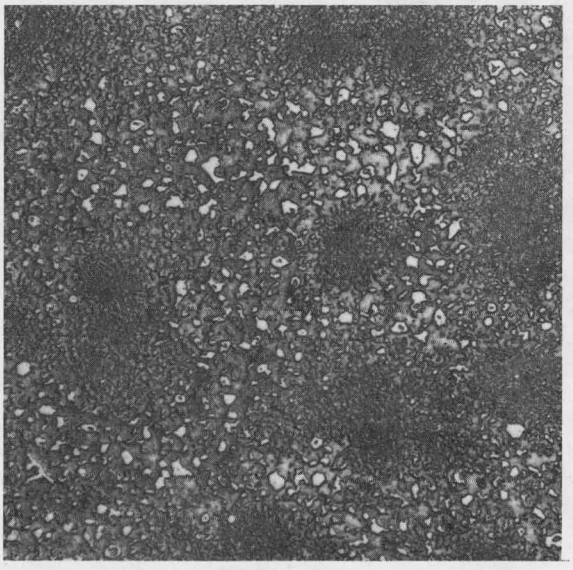

d) 27Cr Normal

Fig.4. Microstructures of a) and b) 15Cr-3 Mo cast iron with Cr_7C_3 carbides in an overtempered martensitic matrix and c) and d) 27Cr (HC-250) cast iron with Cr_7C_3 carbides in a matrix of lightly tempered martensite. 100X.

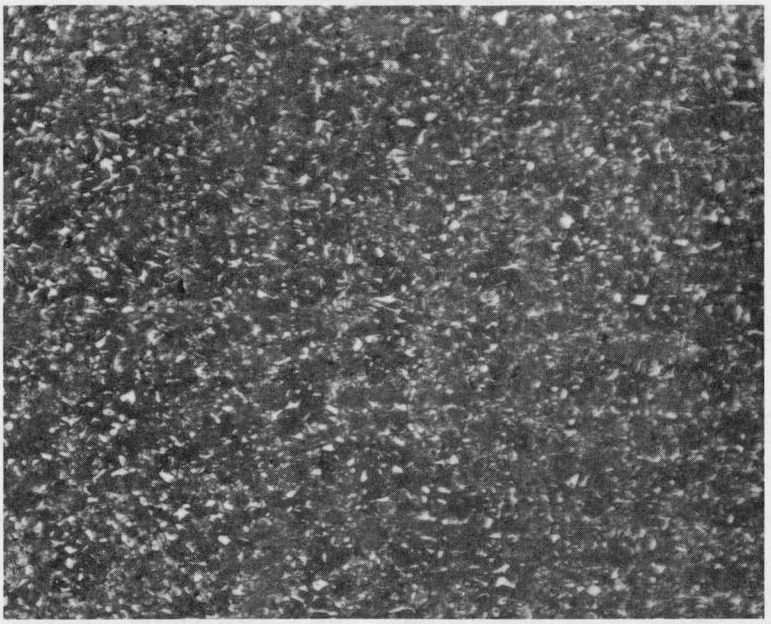

90X

360X

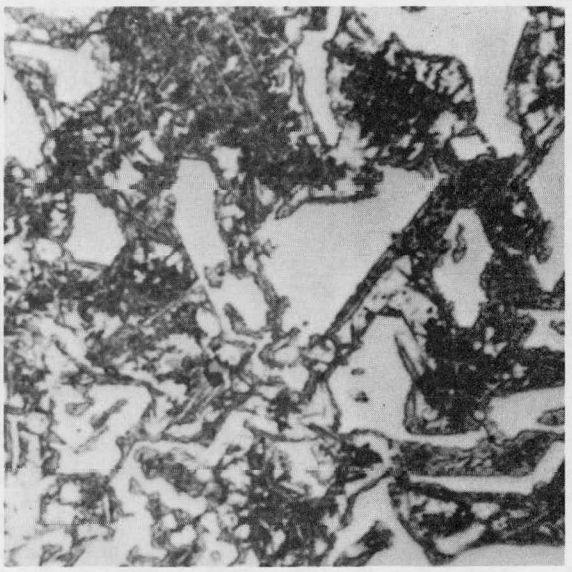

960X

Fig.5. Microstructure of Ni-Hard 4 cast iron with 40 percent retained austenite. M_7C_3 carbides in a matrix of tempered martensite and 40 percent retained austenite.

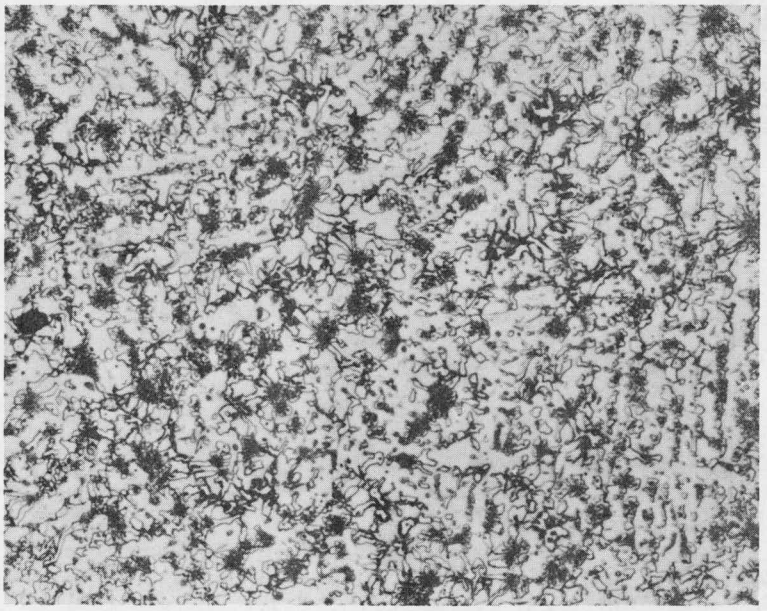

90X

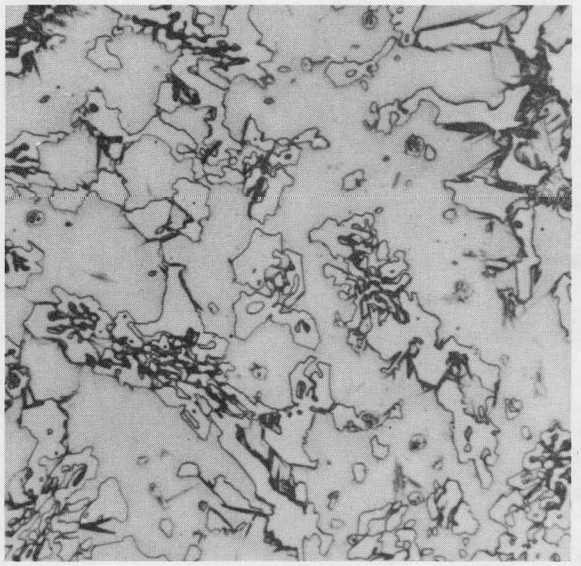

360X

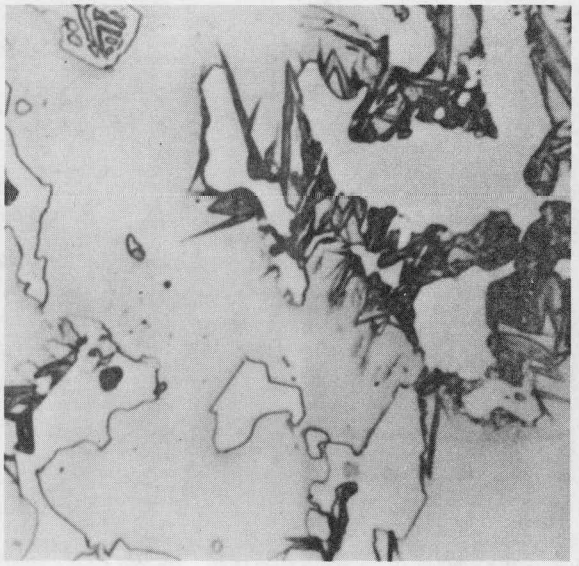

960X

Fig.6. Microstructure of Ni-Hard 4 cast iron with 85 percent retained austenite. M_7C_3 carbides in a matrix of tempered martensite and 85 percent retained austenite.

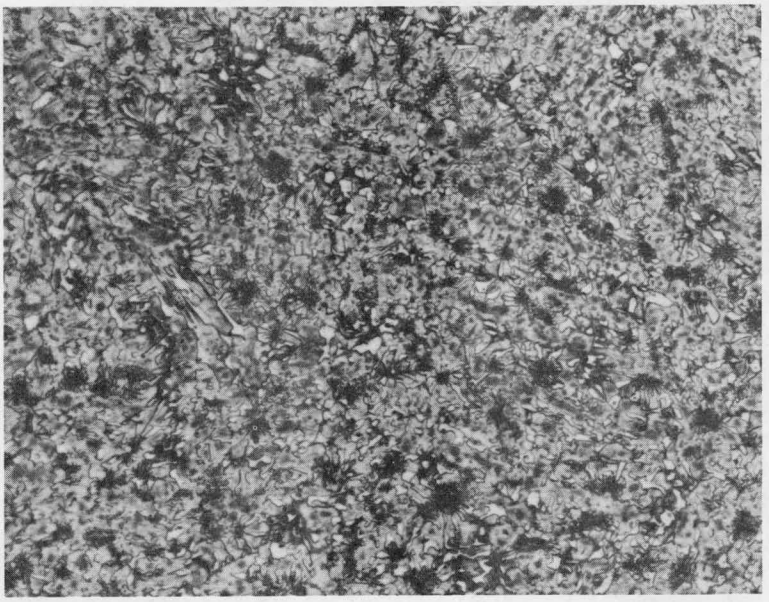

90X

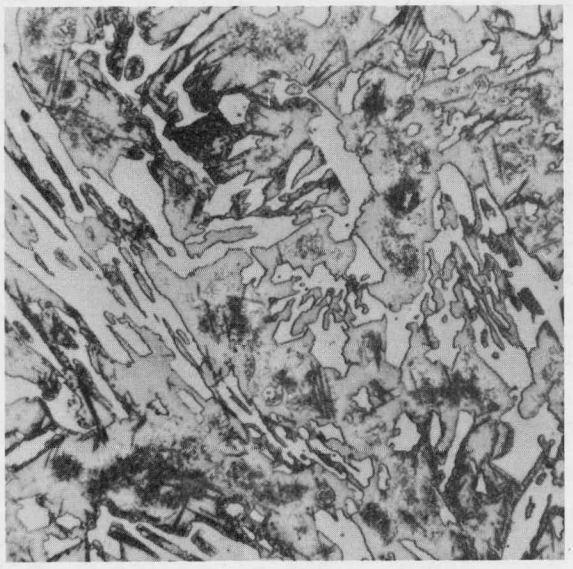

360X

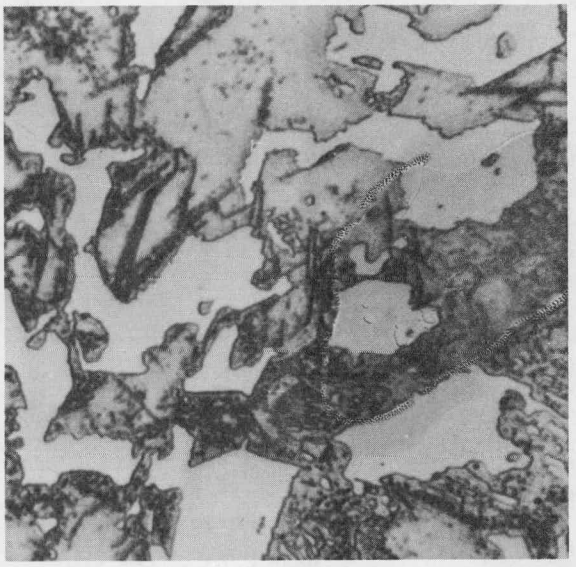

960X

Fig.7. Microstructure of Ni-Hard 4 cast iron with 5 percent retained austenite. M_7C_3 carbides in a matrix of tempered martensite and 5 percent retained austenite.

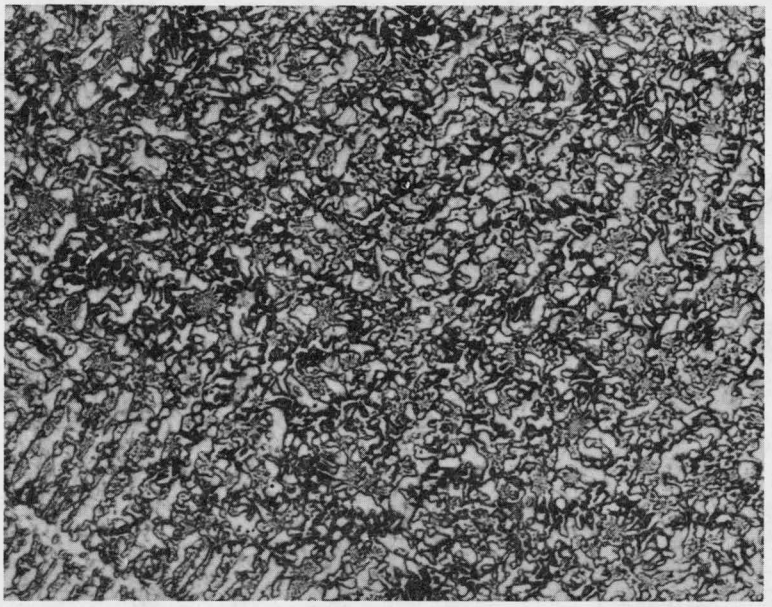

90X

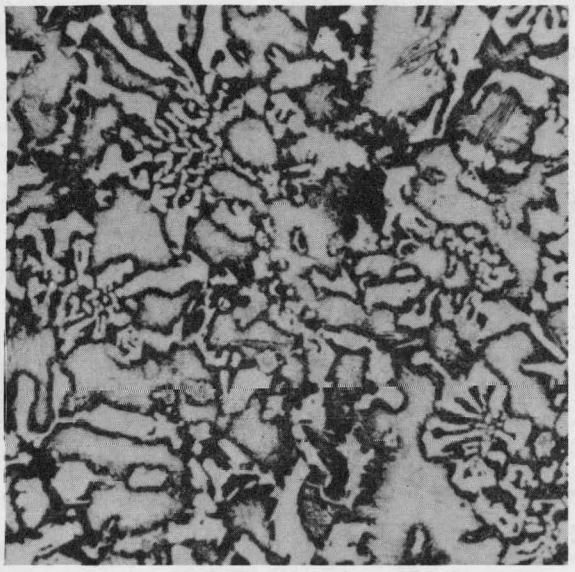

360X

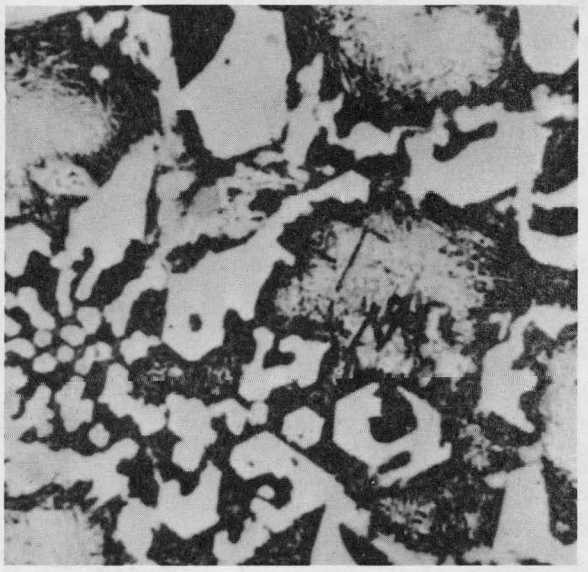

960X

Fig.8. Microstructure of Ni-Hard 4 cast iron with 20 percent retained austenite. M_7C_3 carbides in a matrix of tempered martensite and 20 percent retained austenite.

Figure 9 shows RWAT weight loss and AMAX pin test (APT) weight loss versus Rockwell C(R_c) hardness of the Ni-Hard 4 irons with 5,20,40 and 85% retained γ in the matrix. Both the RWAT and APT results indicate that minimum wear resistance occurs at 40% retained γ. This result was discussed in quarterly report COO-4246-2, and now that wear testing of the irons has been completed, effort will be directed toward developing an understanding of this behavior.

In Figure 10, the GAWT abrasion factor is plotted against R_c hardness, and it is apparent that maximum wear resistance (minimum AF) occurs at 40% retained γ. As with the minimum resistance observed in the RWAT, reasons for the maximum in GAWT wear resistance are currently under study.

It is not unusual for the relative wear resistance of various microstructural forms of a given material to change as wear test conditions are altered. For example, Grunlach and Parks [4] have reported that high Cr irons have maximum wear resistance in the austenitic form when run against SiC (KHN 2100) or Al_2O_3 (KHN 1650) abrasives in the APT. When run against a softer abrasive, garnet (KHN 750), they display maximum resistance in the martensitic condition. It is hoped that scanning electron micrograph (SEM) analysis of RWAT and GAWT wear scars and the metallographic analysis through the deformed layer of the Ni-Hard 4 samples will provide information which will lead to developing mechanisms for this behavior.

2.4 Task IV Wear Scar and Microstructure Characterization

Work on the QTM portion task has just begun. Included in this report as Appendix I is a summary prepared by Mr. Joseph Coyle, graduate research assistant, of the potential use of QTM to establish microstructure-wear resistance relations.

The standard metallography has been completed on all of the cast irons listed in Table I, and characterization of wear scars will be undertaken in the next quarter.

2.5 Task V Analysis of Data

As the proposal and the Work Statement for the project indicate, analysis of the data requires comparison of results from three separate sets of measurements: RWAT and GAWT weight loss tests; mechanical tests including macro and microhardness; metallographic studies which include standard metallography, QTM, and wear scar characterization by SEM and microtopography. The analysis process is to proceed in two steps. First, an attempt is to be made to correlate empirically RWAT and GAWT weight loss behavior to various mechanical properties and metallographic parameters. Second, in cases where empirical correlations exist, attempts are to be made to interpret them in terms of basic theories of mechanical behavior; viz. theories involving dispersion strengthening or work hardening. The purpose of the first step in the analysis is to develop empirical rules for materials' selection and/or alloy design for wear resistance. The purpose of the second step is to improve understanding of the basic phenomena of abrasive wear which in turn may lead to an improved fundamental approach in materials' selection and/or alloy design.

Essentially all of the RWAT and GAWT wear testing of the cast irons has been completed. In the mechanical test phase of Task V, macro and microhardness measurements have been correlated empirically to wear resistance. Correlation

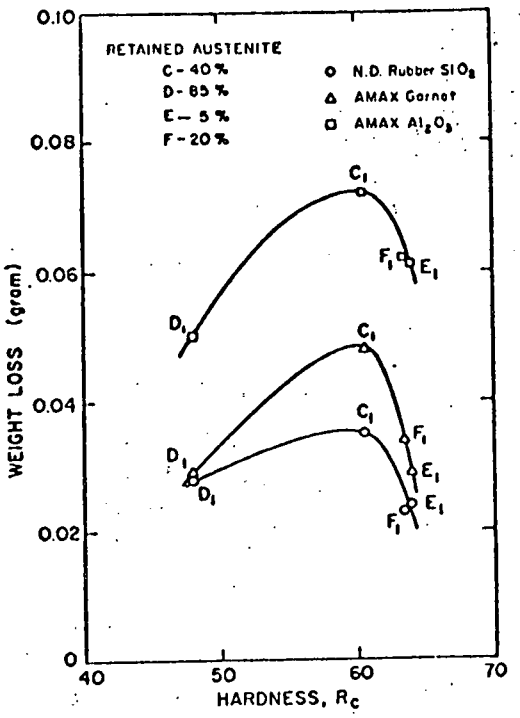

Figure 9. The effect of hardness and percent retained austenite on the wear of Ni-Hard 4 cast irons tested at Notre Dame (RWAT) and Amax (pin test) laboratories.

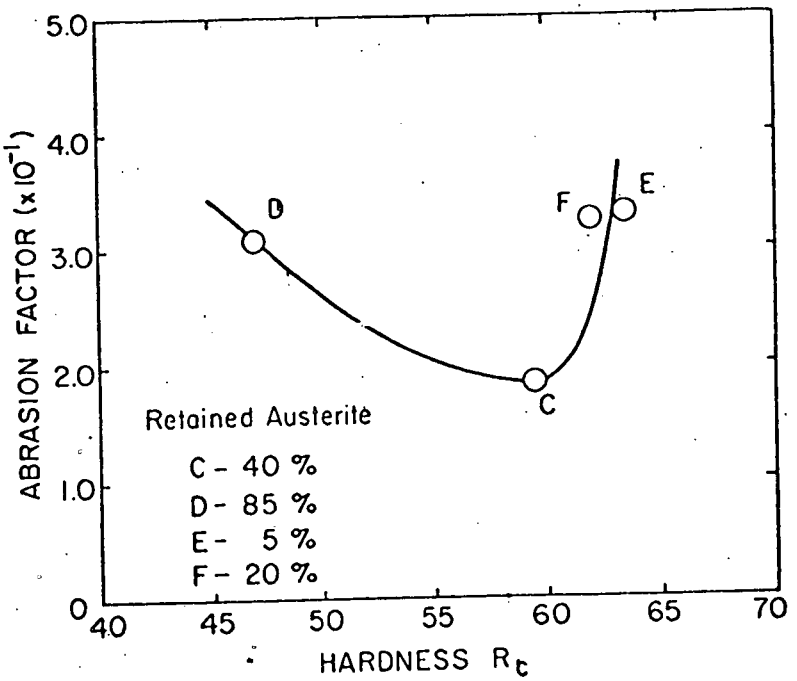

Figure 10. The effect of hardness and percent retained austenite on the abrasion factor of Ni-Hard 4 cast irons tested in the GAWT.

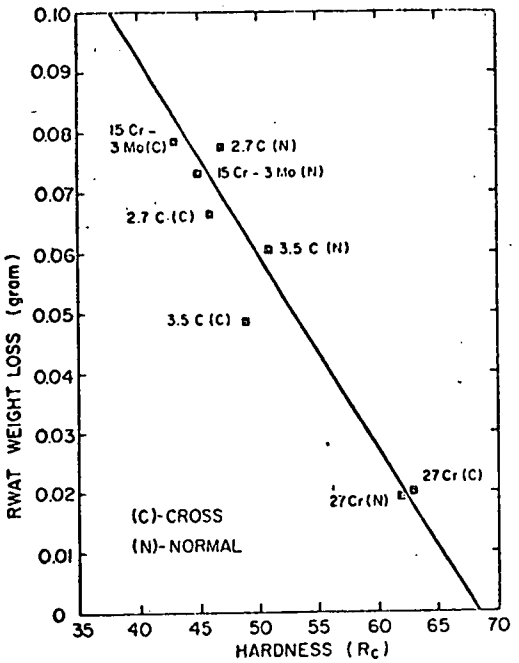

Figure 11. The relationship between RWAT weight loss and macrohardness of a 3.5C and a 2.7C pearlitic cast iron, a 15Cr-3Mo cast iron and a 27Cr cast iron tested in two orientations.

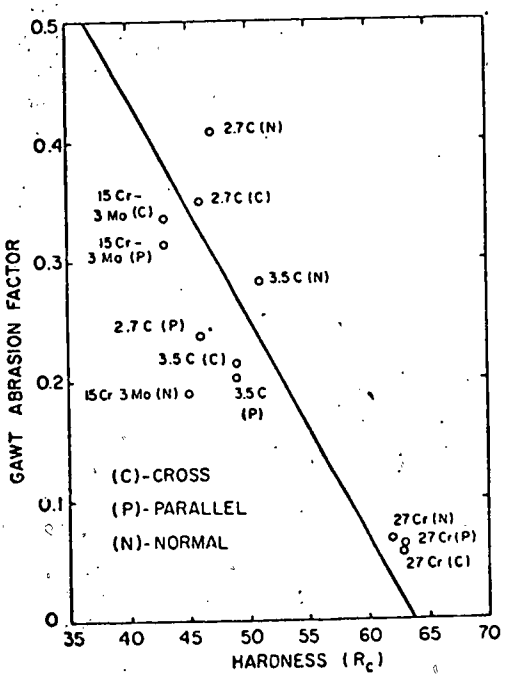

Figure 12. The relationship between the GAWT abrasion factor and macrohardness of a 3.5C and a 2.7C cast iron, a 15Cr-3Mo cast iron and a 27Cr cast iron each tested in three orientations.

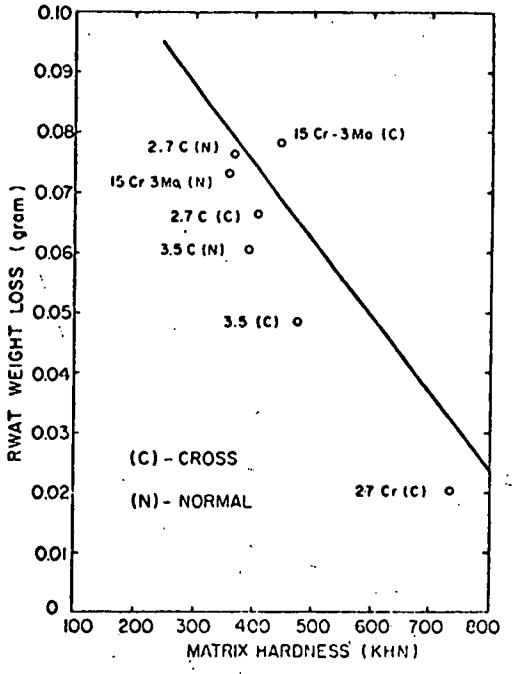

Figure 13. The relationship between RWAT weight loss and the matrix hardness for four white cast irons tested in two orientations.

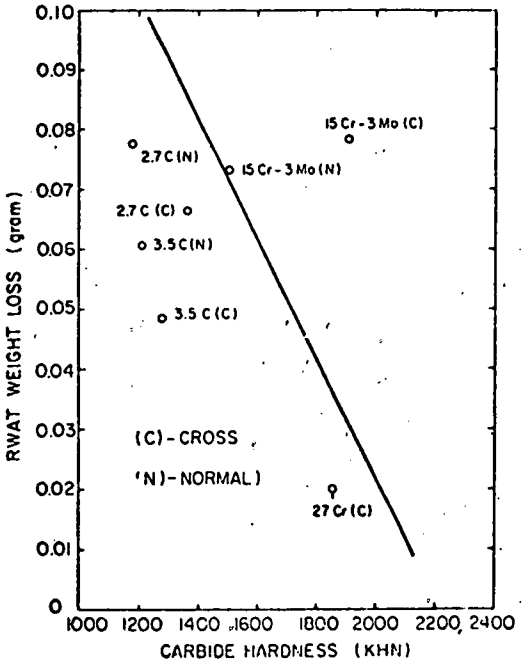

Figure 14. The effect of carbide hardness on the RWAT weight loss for four white cast irons tested in two orientations.

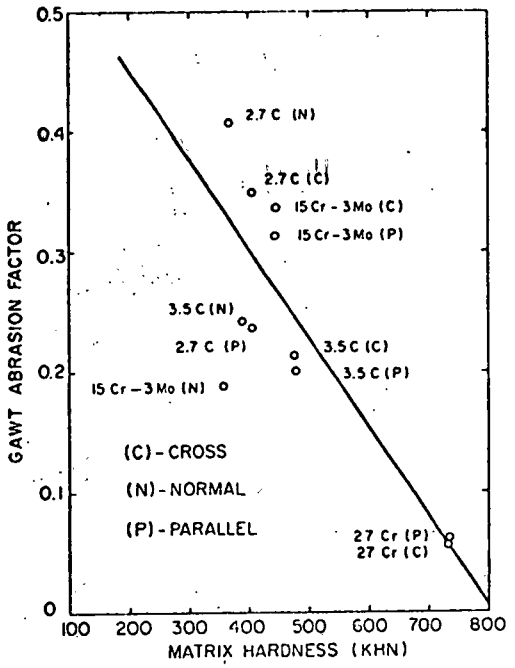

Figure 15. The relationship between the GAWT abrasion factor and matrix hardness for four white cast irons tested in three orientations.

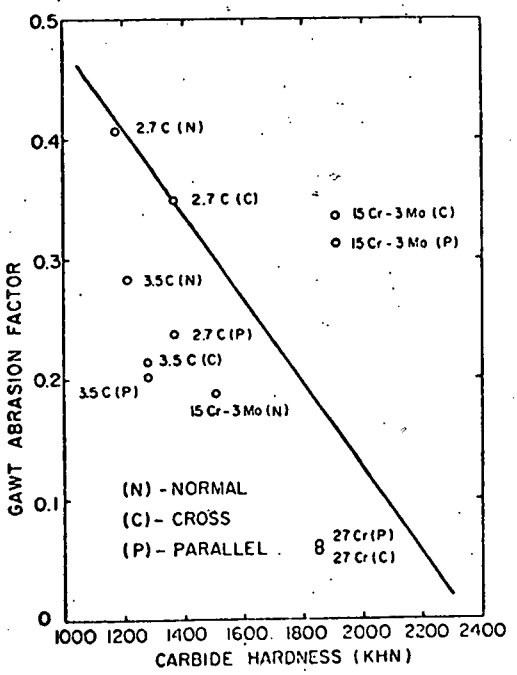

Figure 16. The effect of carbide hardness on the GAWT abrasion factor for four white cast irons tested in three orientations.

of additional mechanical properties to wear resistance may be made only for Ni-hard 4, since this is the only iron which exists in a sufficient number of microstructural states to allow generation of meaningful correlations. In the following sections of the report, progress in developing empirical wear-hardness, wear-property and wear-microstructure generalizations will be described.

2.5.1 Empirical Wear-Hardness Correlations

As may be seen from Figures 10 and 11, both RWAT and GWAT wear resistance fail to correlate simply with macrohardness for the Ni-hard 4 irons. The reasons for the existence of the maximum in GAWT wear resistance and the minimum in RWAT wear resistance at 40% retained γ may become apparent as the more basic microstructural studies progress.

It is also difficult to develop wear-microhardness correlations for the Ni-hard 4 specimens since carbide hardness is constant at about 1950 KHN for all four microstructural states, but "matrix microhardness" becomes undefinable in these materials, whose matrix consists of discrete zones of a very soft consituent (retained γ) intermingled with zones of a hard constituent (tempered martensite).

On the other hand, it is evident from Figures 11 through 16, that valid attempts may be made to correlate RWAT and GAWT to macrohardness, carbide microhardness and matrix microhardness in the two pearlitic white irons, in 15Cr-3Mo and in the 27Cr iron. It is rather straight-forward to make qualitative empirical correlations for these materials. For example, RWAT weight loss appears to correlate more closely with R_c macrohardness (Figure 11) than does GWAT weight loss (Figure 12). The generalizations may be made more quantitative by application of the graphical statistical method described by Johnson [5]. Space is taken to outline this method here because it is rather simple to perform, yet sheds much light on wear-hardness correlations.

Let (x_1,y_1), (x_2,y_2), ... (x_n,y_n) correspond to n measurements of some property y_i which is thought to be a function of some parameter x_i. For example the y_i may be the RWAT weight loss measurements displayed in Figure 9, and the x_i may be the R_c hardness corresponding to each weight loss. A least squares line may be drawn through <u>any</u> such set of (x_i,y_i), although the data are so scattered that no real physical correlation may exist between x and y. The equation of the line is

$$y = b_1 x + b_o, \tag{1}$$

where

$$b_o \frac{(\Sigma y_i)(\Sigma x_i^2) - (\Sigma x_i)(\Sigma x_i y_i)}{n(\Sigma x_i^2) - (\Sigma x_i)^2}, \tag{2}$$

and

$$b_1 = \frac{n(\Sigma xy) - (\Sigma x)(\Sigma y)}{n(\Sigma x^2) - (\Sigma x)^2}. \tag{3}$$

From this set of data, a linear correlation coefficient r may be calculated such that

$$r = \frac{n(\Sigma x_i y_i) - (\Sigma x_i)(\Sigma y_i)}{\sqrt{n(\Sigma x_i^2) - (\Sigma x_i)^2}\ \sqrt{n(\Sigma y_i^2) - (\Sigma y_i)^2}} \qquad (4)$$

A perfect correlation exists between y and x if $r = \pm 1$. If for the n observations, $|r \text{ (calculated)}| > |r_n|$, the correlation is satisfactory. Here r_n is a critical value of r such that a decision based on the criterion $|r \text{ (calculated)}| > |r_n|$ will have at least 0.9 probability of being correct. In Table III are displayed values of r_n corresponding to various values of observation, n. As n increases, lower values of r_n suffice to indicate linear correlation.

Table III

Critical Linear Correlation Coefficients for n Observations

n	r_n
5	0.878
6	0.811
7	0.754
8	0.707
9	0.666
10	0.632
15	0.514
20	0.444
30	0.361
50	0.279
100	0.196

Computation of b_1, b_o and r is somewhat cumbersome, and these quantities usually may be estimated by a simplified technique consisting of the following steps:

1. Plot the n datum points (x_i, y_i)
2. Draw as compact as ellipse as possible around the points.
3. Measure the minor axis d and the major axis D; then

$$r \cong 1 - d/D \qquad (5)$$

$b_1 \cong$ slope of major axis

$b_o \cong$ y intercept of major axis

This graphical technique has been applied to the data shown in Figures 11 through 16, and the results are summarized in Table IV. A number of empirical generalizations are suggested by these results:

Table IV.

Tests of Correlation: Wear to Hardness

Condition	n	d/D	r	r_n	Remarks
RWAT to Macrohardness	8	.169	.831	.707	Correlation exists
GAWT to Macrohardness	12	.289	.711	.576	Correlation exists
RWAT to Matrix Microhardness	7	.175	.825	.754	Correlation exists
RWAT to Carbide Microhardness	7	.479	.521	.754	No correlation
GWAT to Matrix Microhardness	11	.313	.687	.602	Correlation exists
GAWT to Carbide Microhardness	11	.425	.575	.602	No Correlation

1. Wear resistance appears to correlate better to macrohardness in the RWAT than in the GAWT. The superior correlation of the RWAT is probably not due to intrinsic differences in reproducibility in the two tests since they have comparable coefficients of variation. Futher, it is not due to the fact that the GAWT include data for cross, normal and parallel specimen orientation and the RWAT only include data for cross and normal, because the parallel data lie within the spread of the cross andnormal data. Rather it appears that the behavior is a true manifestation of microstructural effects,and that hardness is a better indicator of wear resistance of cast irons in low-stress abrasion applications than in gouging applications. It may indicate that the hardness test, which in effect is a measure of matrix yielding in compression,simulates low-stress wear more closely than it does gouging wear which may involve impact, matrix yielding and carbide fracture. This is an important result in that it may lead to more effective predictive techniques for wear resistance.

2. For both the RWAT and GAWT results, wear resistance correlates to matrix microhardness (in the alloys of relatively homogeneous matrices), whereas it does not correlate to carbide microhardness.

This generalization may also have metallurgical value in that it suggests that for a range of abrasive hardness and stress conditions, emphasis should be placed on alloying and processing to optimize matrix properties of white irons.

2.5.2 Other Empirical Wear-Property Correlations

The Ni-Hard 4 materials have been subjected to extensive mechanical testing at the Climax Molybdenum Research Laboratories [6,7]. Emphasis has been placed on tests which provide gauges of toughness. The mechanical testing program consisted of the following:

1. Slow strain rate compression measurements of compression yield strength σ_y and compression ultimate fracture strength σ_u. Compressive shear strength σ_s was calculated by multiplying σ_u by the sine of the angle between the compression axis and the plane along which the samples fractured.

2. Rolling fatigue tests in which cylindrical specimens were rotated and compressed at a frequency of 1700 Hz by a cluster of three work rolls. These tests generated rolling fatigue endurance limit σ_{EF}, rolling fatigue Hertzian fracture strength σ_{HE} and maximum shear strength at fatigue fracture σ_{SF}.

3. Impact bending tests under single-and repeated-impact conditions which generated impact-bend tensile strength for single impact σ_I and impact-bend tensile strength for repeated impact σ_{IR}.

4. Plain-strain fracture toughness tests, which generated fracture toughness K_{IC}.

RWAT weight loss and GAWT Abrasion Factor are plotted against these nine mechanical properties in Figures 17 through 23 in an effort to reveal wear-property correlations. Several generalizations follow from these plots:

1. Correlations involving σ_{EF}, σ_{HF}, σ_{SF}, σ_I, σ_{IR} and K_{IC} are no better than those involving hardness, σ_y, σ_u and σ_s. Since determination of the former quantities require elaborate testing procedures, it is doubtful that their use as predictive tools is justified. Whether they have value in elucidating wear mechanisms however, may be ascertained only after the in-depth metallographic and topographic studies are complete.

2. In general, values of properties which indicate high RWAT wear resistance indicate low GAWT wear resistance. Similarly, cases in which the RWAT-property plot passes through a maximum at a certain value of the property correspond to cases in which the GAWT-property plot passes through a minimum at the same value of the property. Thus the inversion in RWAT property and GAWT property behavior identified in the hardness correlations persists through the other property correlations. This may simply underscore the fact that the RWAT and GAWT produce two distinct mechanisms of abrasion.

3. The RWAT and GAWT wear correlations involving σ_u or σ_s offer an advantage over those involving σ_y or hardness, since they are monotonic without extremal points. This has an advantage from a predictive viewpoint since wear resistance is a smooth single function of the two technical properties.

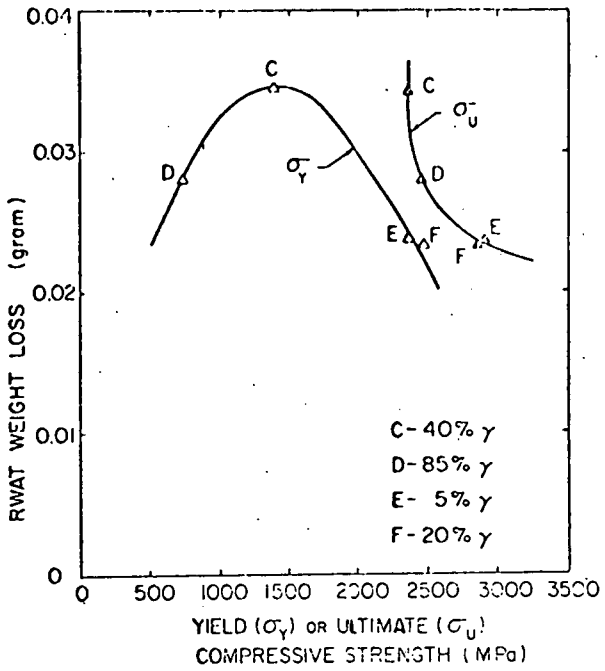

Figure 17. The effect of yield (σ_y) and ultimate (σ_u) compressive strength on the RWAT weight loss for Ni-Hard 4 cast irons.

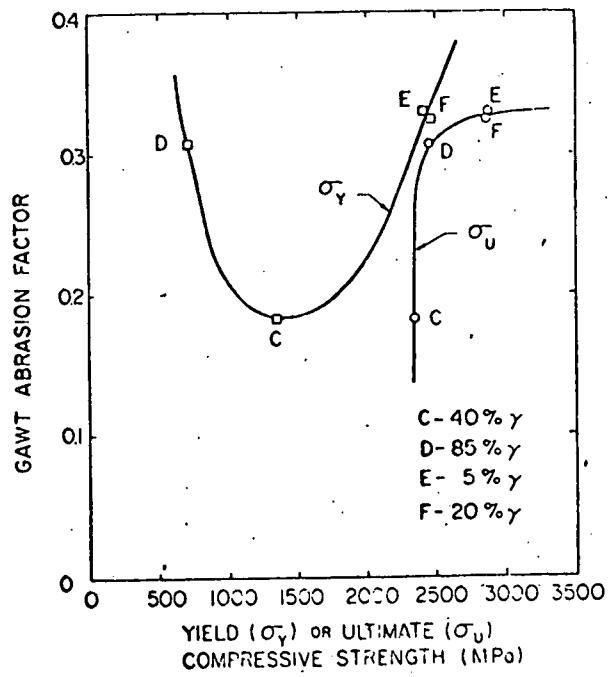

Figure 18. The effect of yield (σ_y) and ultimate (σ_u) compressive strength on the GAWT abrasion factor for Ni-Hard 4 cast irons.

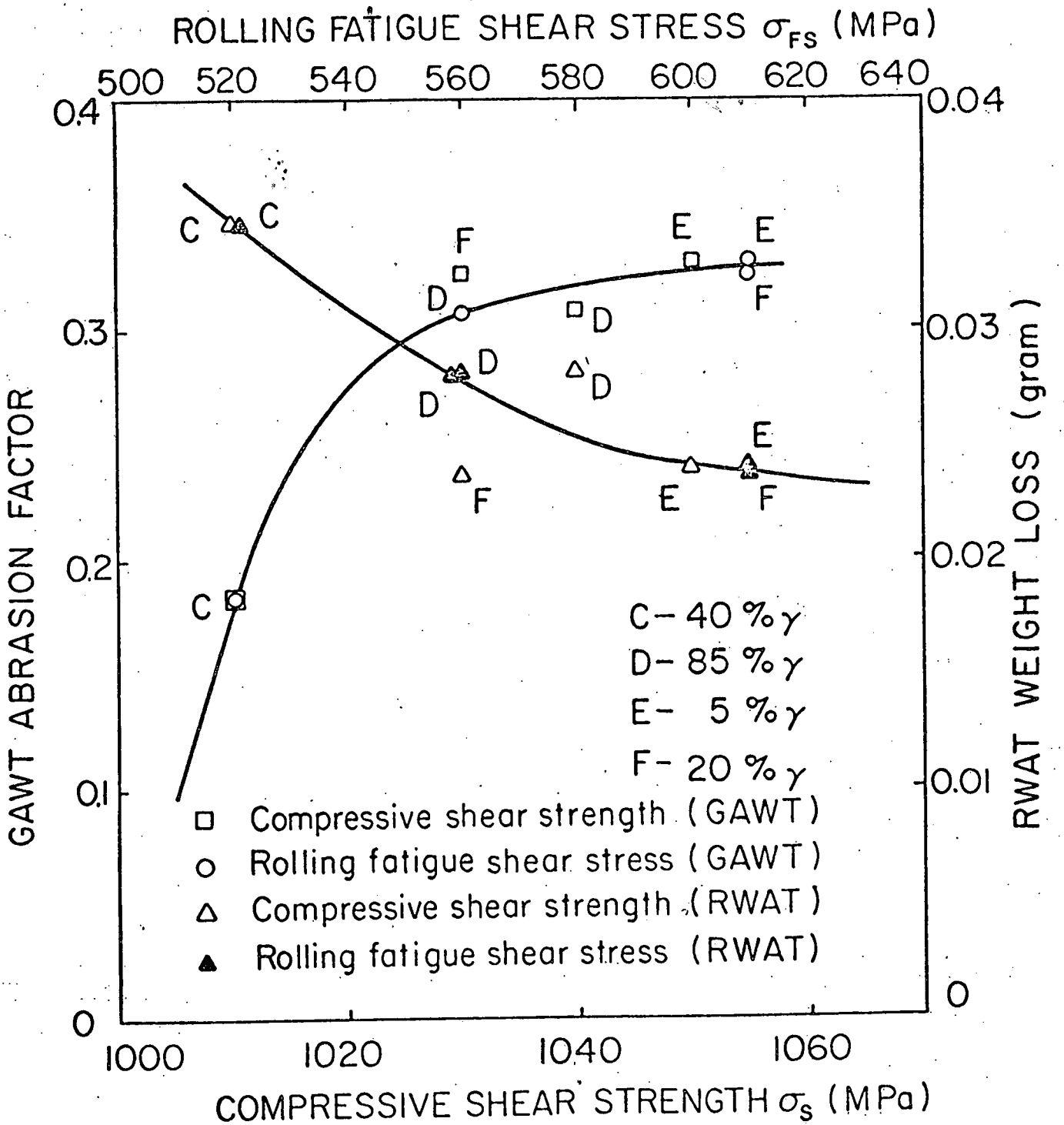

Figure 19. The effect of rolling fatigue (σ_{FS}) and compressive (σ_S) shear strength on the RWAT weight loss and the GAWT abrasion factor for Ni-Hard 4 cast irons.

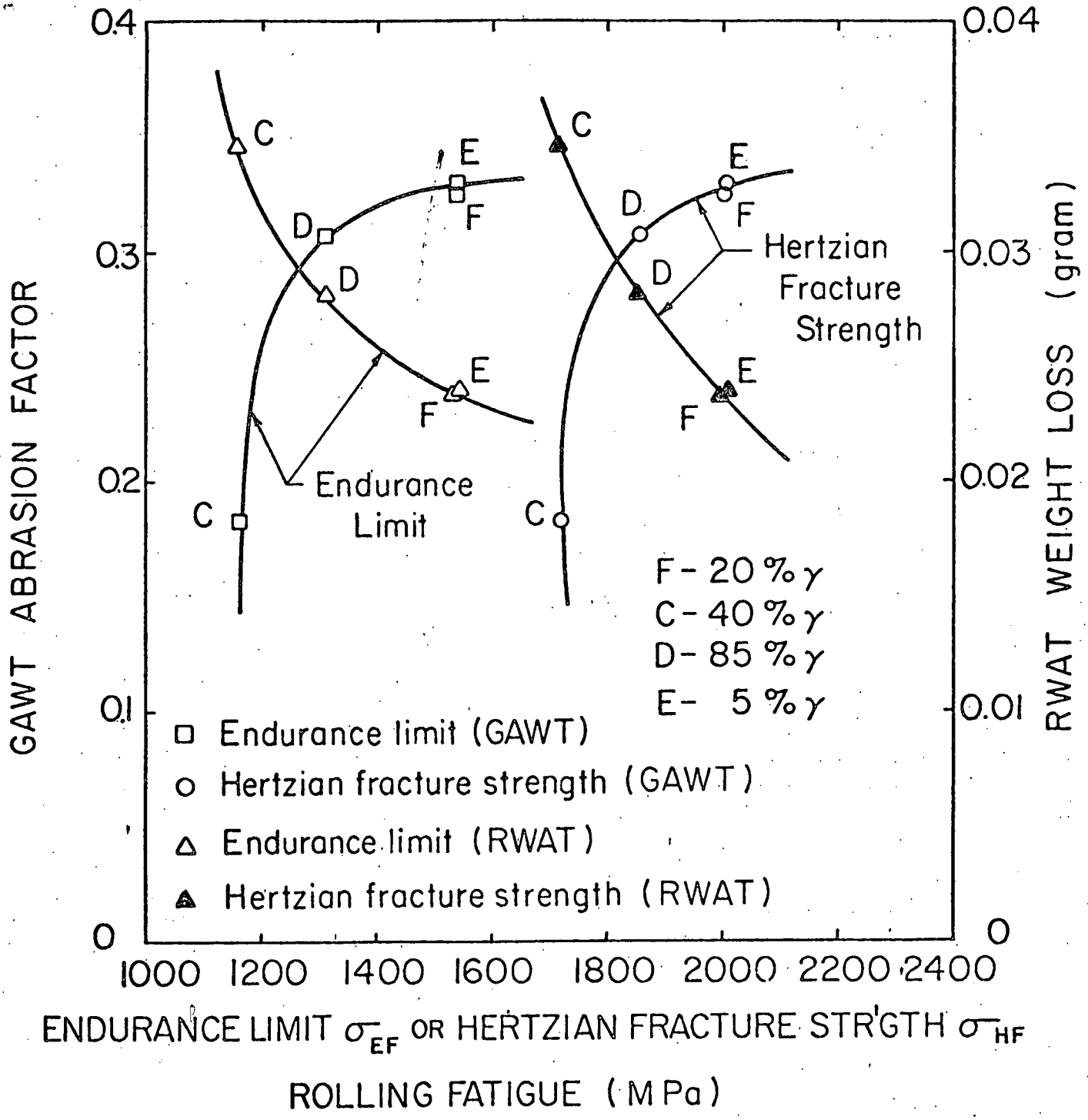

Figure 20. The effect of rolling fatigue endurance limit (σ_{EF}) and Hertzian fracture strength (σ_{HF}) on the RWAT weight loss and the GAWT abrasion factor for Ni-Hard 4 cast irons.

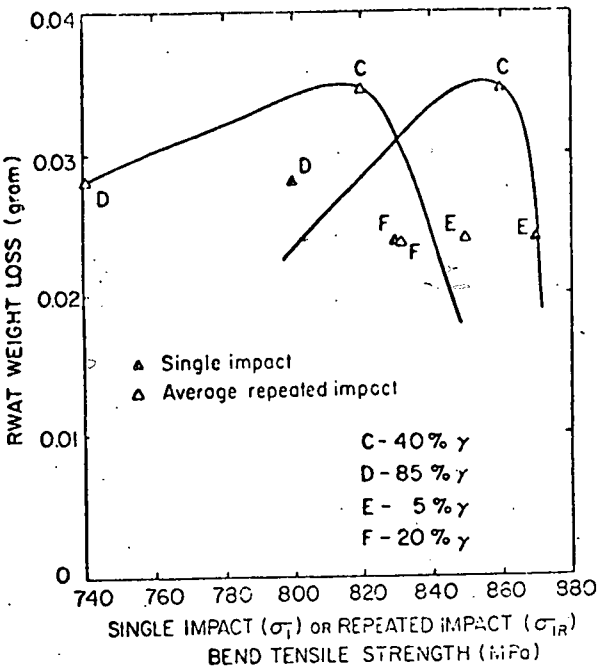

Figure 21. The effect of single impact (σ_I) and repeated impact (σ_{IR}) bend tensile strength on RWAT weight loss for Ni-Hard 4 cast irons.

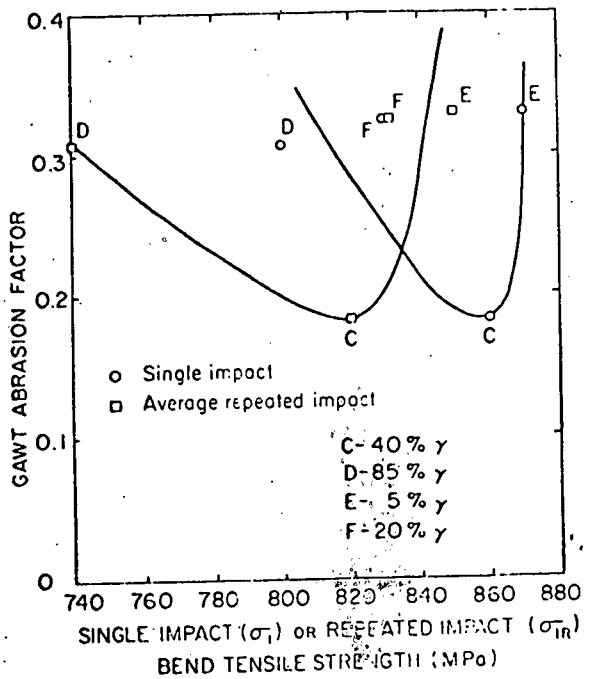

Figure 22. The effect of single impact (σ_I) and repeated impact (σ_{IR}) bend tensile strength on the GAWT abrasion factor for Ni-Hard 4 cast irons.

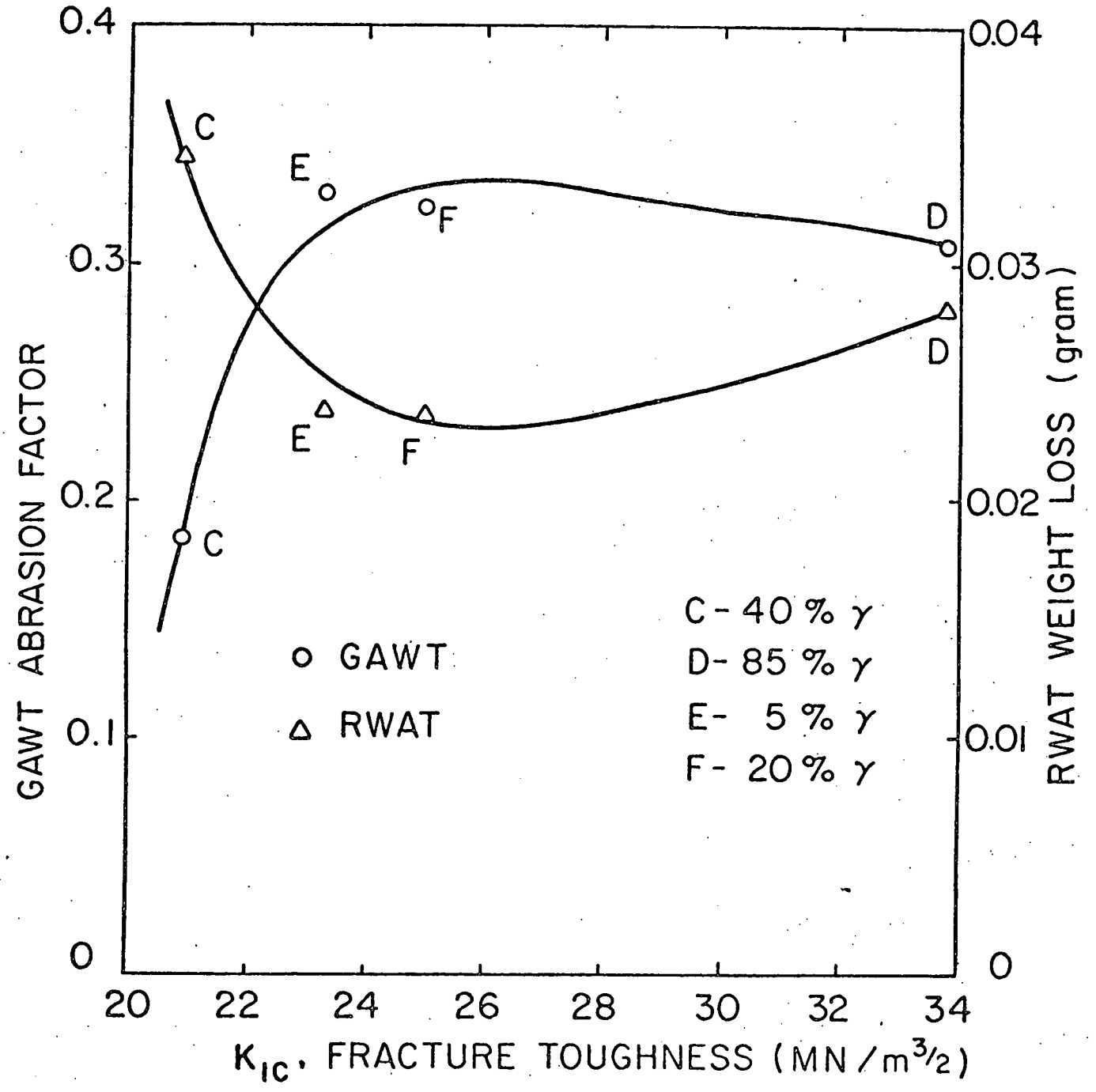

Figure 23. The effect of fracture toughness on the RWAT weight loss and the GAWT abrasion factor for Ni-Hard 4 cast irons.

3. SUMMARY

In general terms, the major objective of this research is the development of rules which will lead to an improved understanding of wear and improved materials for resisting wear. A number of such general rules appear to be evolving from the research, although the program has just reached the point where in-depth study is commencing. These preliminary rules, quite tentative in nature, are summarized in this section of the report.

1. In alloy white irons, wear resistance is a strong function of such parameters as carbide volume fraction, carbide shape and matrix strength. Situations readily arise in which the effort and expense of alloying is wasted because the various effects of such microstructural parameters on wear are not balanced.

2. In the Ni-Hard 4 irons, retained austenite may improve or may decrease wear resistance depending on its relative amount and the type of wear under consideration.

3. In the Ni-Hard 4 irons, macro or micro hardness is not as good a gauge of wear resistance as is compressive shear or ultimate strength.

4. In the irons other than the Ni-Hards, macrohardness and matrix microhardness are good gauges of RWAT and GAWT wear resistance. Carbide microhardness is not, which may indicate that for white irons, more emphasis should be placed on alloying and processing to optimize matrix properties.

5. In the irons other than the Ni-Hards, macrohardness and matrix microhardness correlate to RWAT wear resistance better than GAWT wear resistance. This may indicate that low-stress abrasion mechanisms may be understood in terms of basic theories of plastic deformation.

6. RWAT and GAWT wear resistance correlate to hardness and compression test properties at least as well as they do to properties which are much more difficult to measure.

4. PERSONNEL

The principal investigator, Dr. N. F. Fiore, has spent about one-fifth effort on the project during this quarter of the academic year. Two graduate students, Mr. Joseph Coyle (Ph.D. candidate) and Mr. Steven Udvardy (M.S. candidate) have devoted half-time effort to the project.

REFERENCES

1. R. C. Tucker, Jr. and A. E. Miller, "Low Stress Abrasive and Adhesive Wear Testing," ASTM STP 615, R. G. Bayer, Ed., (ASTM, Philadelphia, 1976) pp. 68-90.

2. H. S. Avery, "Classification andPrecision of Abrasion Tests," Int. Conf. on Wear of Matls., St. Louis, 1977.

3. ASTM Manual on Quality Control, ASTM STP 15-C, (ASTM, Philadelphia, 1951), pp. 1-50.

4. R. B. Grundlach and J. L. Parks, "Influences of Abrasive Hardness on Wear Resistance of High Cr Irons," Internatl. Conf. on Wear of Materials, St. Louis, 1977. (Climax Molybdenum Research Laboratories, Ann Arbor, MI Report L-212-155, 1977).

5. R. Johnson, Elementary Statistics (Duxbury Division, Wadsworth Publishers, Belmont, CA, 1973) Ch. 3.

6. D. E. Diesburg, "Performance of Abrasion Resistance Irons in Laboratory Tests" (Climax Molybdenum Research Laboratories, Ann Arbor, MI Report L-212-138, 1975).

7. D. E. Diesburg and F. Borik, "Optimizing Abrasion Resistance and Toughness," Proc. of Symp. on Materials for the Mining Industry, (Climax Molybdenum Company, 1974).

LIST OF TABLES

LIST OF FIGURES

Figure 15. The relationship between the GAWT abrasion factor and matrix hardness for four white cast irons tested in three orientations.

Figure 16. The effect of carbide hardness on the GAWT abrasion factor for four white cast irons tested in three orientations.

Figure 17. The effect of yield (σ_y) and ultimate (σ_u) compressive strength on the RWAT weight loss for Ni-Hard 4 cast irons.

Figure 18. The effect of yield (σ_y) and ultimate (σ_u) compresive strength on the GAWT abrasion factor for Ni-Hard 4 cast irons.

Figure 19. The effect of rolling fatigue (σ_{ES}) and compressive (σ_S) shear strength on the RWAT weight loss and the GAWT abrasion factor for Ni-Hard 4 cast irons.

Figure 20. The effect of rolling fatigue endurance limit (σ_{EF}) and Hertzian fracture strength (σ_{HE}) on the RWAT weight loss and the GAWT abrasion factor for Ni-Hard 4 cast irons.

Figure 21. The effect of single impact (σ_I) and repeated impact (σ_{IR}) bend tensile strength on RWAT weight loss for Ni-Hard 4 cast irons.

Figure 22. The effect of single impact (σ_I) and repeated impact (σ_{IR}) bend tensile strength on the GAWT abrasion factor for Ni-Hard 4 cast irons.

Figure 23. The effect of fracture toughness on the RWAT weight loss and the GAWT abrasion factor for Ni-Hard 4 cast irons.

COO-4246-3

APPENDIX I

QUANTITATIVE METALLOGRAPHY - ITS POTENTIAL USE IN WEAR-MICROSTRUCTURE STUDIES

by

Joseph P. Coyle

University of Notre Dame

D.O.E. Project EF 77-S-02-4264

January, 1978

INTRODUCTION

For years scientists have been involved in the fundamental study of relating materials' structures and properties. Recent trends favor quantitative correlations between the two not only on a microscopic but also on a macroscopic level, by means of quantitative image analysis. Two groups especially interested in the latter are materials scientists and metallurgical engineers, who in their own disciplines attempt to understand both structures and properties of materials and metals respectively. Now there is need for connecting the two so that properties can be quantitatively predicted by observing the structures and vice versa, i.e., the structures can be quantitatively described from the property measurements. In order to be successful, both will have to command a basic understanding of quantitative image analysis.

CHARACTERISTIC QUANTITIES OF MICROSTRUCTURE

In quantitative microscopy, structure is generally described in terms of the "global parameters of microstructure" which are listed in Table I, [1,4,5]. These can be related to material properties in two ways. First, they relate directly to material physical properties which are additive, e.g., the correlation between phase volume fraction (V) and density (ρ) in a two phase alloy [1],

$$\rho_{Alloy} = \rho_{\beta} + (\rho_{\alpha} - \rho_{\beta})V_{\alpha} .$$

In a plain carbon steel ρ and V relate to composition as [1]

$$\% \text{ Carbon} = \frac{(0.0677\ (V_{\beta} \cdot \rho_{\beta})}{(1-V_{\beta})\ \rho_{\alpha} + V_{\beta}\rho_{\beta}} ,$$

where β is Fe_3C and α is α-Fe. Another example is the relationship between hardness and the amount of phase interface(s) in a two phase alloy [1],

$$\text{Hardness (BHN)} = a + kS \quad , \quad \text{where}$$

a is the BHN for a one-phase alloy (matrix) and k is a slope constant. The Hall-Petch equation relates grain size to yield strength [3],

$$\sigma_{y.s.} = A + Bd^{-1/2}$$

where A and B are constants and d is the grain size.

Secondly, ratios of one global parameter to another are quantities that sometimes relate to average material properties. For example, the mean free path in a two phase alloy (τ) is given by [1],

$$\tau = \left(\frac{4V_{\alpha}}{S_{\alpha}}\right).$$

The global parameters are the basic quantities which are measured, and the five listed in Table I are the most applicable to common metallurgical problems. There are other parameters which are used for quantitatively describing microstructure geometry, such as the Feret's diameter, perimeter and "homemade" quantities [3] such as contiguity (C),

$$C = \frac{2S_{\alpha\alpha}}{2S_{\alpha\alpha}+S_{\alpha,\beta}} = \frac{4\bar{L}_{\alpha}^{2}}{\bar{L}_{\alpha}^{2} + 4A_{\alpha}} \quad , \quad \text{where}$$

$S_{\alpha\alpha}$ = surface interface between phase α ,

$S_{\alpha,\beta}$ = surface interface between α and β phases,

$\bar{L}_{\alpha}$ = mean intercept length of phase α and

A_{α} = area of phase α per unit area.

The transverse rupture strength of WC/Co was found to be inversely proportional [3] to $\underset{\sim}{C}$. Another "homemade" parameter, a "shape factor" (R),

$$R_{\alpha} = \frac{A_{\alpha}}{p_{\alpha}} \quad ,$$

where R is the roundness of phase α particles and p_{α} is the perimeter of phase α , was used by Muscara [6] to explain wear trends in white cast irons.

Therefore a study which correlates microstructure and properties should include the following measurements:

1) The global parameters. These should be combined and related to the properties either directly or in ratios.

2) Special parameters already developed by other scientists.

3) "Homemade" parameters to fit special interests, which are often necessary in new areas of study.

SAMPLE PREPARATION

In order to obtain accurate, reproducible measurements in quantitative image analysis, sample preparation is of prime importance. It should include the following steps:

Examination

1) The surface should be planar and flat.

2) The surface roughness should be minimized.

3) Relief polishing should be negligible.

4) Etching procedures should be for

a) maximum contrast
b) minimum relief
c) minimum over or under etching, and
d) phase staining for maximum contrast, especially in multiphase alloys.

Surface Selection

The surface should be representative of the bulk material. This becomes more important as the inhomogeneity and the directionality of the structure increases.

Statistics

Measurements should be made ten times on each field of view; ten different fields of view should be examined. From these data the following statistical values should be determined:

1) Standard deviation,

2) Variance,

3) Mean values and

4) Percent error.

It is assumed that if all metallographic samples are taken from wear test areas then one sample will sufficiently represent the whole material. Since measurement error increases with the number of operators, only one operator should collect all data.

Table I. Some Global Parameters of Microstructure

Parameter[a]	Symbol	Measurement[b]
Length of Line	L	Direct
Area of Surface	S	Direct
Volume Fraction	V,A,L,p	Direct
Connectedness	G	Manual Measurement
Number[c]	N	Direct

[a]Usually given per unit volume of material.

[b]On a Bausch and Lomb Quantitative Image Analyzer.

[c]Includes number and size distributions of particles.

EXPERIMENTAL PROCEDURES

Cast Irons

The following procedure will be followed to quantitatively describe the microstructures of cast irons:

I. Metallographic Sample Preparation

1) Section samples near wear scar sites.
2) Mount samples in bakelite.
3) Polish samples.
4) Etch surfaces with 2% Nital (low Cr-alloys) or Villella's etch (high Cr-alloys).

II. Direct Measurements on a Bausch and Lomb Omnicron Alpha Image Analysis System.

1) The projected length of the carbide phase per unit area, L_α, which is related to the carbide-matrix interfacial area.
2) The area of the carbide phase per unit area, A_α.
3) Ferets diameter of the carbide phase for N eutectic-type carbides, F_α. F/N is the average carbide size.

III. Calculated Parameters[d]

1) The volume fraction of carbide phase per unit volume,

$$V_\alpha = A_\alpha^{(1,2)} .$$

2) The perimeter (P) of the carbide particles is $L_\alpha(\frac{\pi}{2})$. From perimeter, a shape factor, roundness (R) can be calculated,

$$R = \frac{A_\alpha}{P_\alpha} = \frac{A_\alpha}{(\frac{\pi}{2})L_\alpha} . \quad (6)$$

3) The contiguity (C) of the carbides is

$$C = \frac{4L_\alpha^2}{L_\alpha^2 + 4A_\alpha} . \quad (3)$$

Co-base Superalloys

The following procedure will be followed to quantitatively describe the microstructures of the Co-base superalloys.

I. Metallographic Sample Preparation.

1) Section samples near wear scar sites.
2) Mount in bakelite.

---

[d]These parameters and quantities can be defined for the carbide, matrix and/or a third phase in the microstructures.

3) Polish samples
4) Electrolytically etch with HCl + H_2O_2, then stain the carbide phases with potassium permanganate, $KMnO_4$.

II. Direct Measurements on a Bausch and Lomb Omnicron Alpha Image Analysis System.

1) The projected length of the carbides per unit area, L_α.
2) The area of carbide phase per unit area, A_α.
3) The size distribution of carbides.
4) The number of carbides per unit area.

III. Calculated Parameters

1) Volume fraction of carbide phase, V_α.

$$V_\alpha = A_\alpha \quad (1,2)$$

2) Determine the mean carbide size from the size distribution curves.
3) The contiguity (C) of the carbides,

$$C = \frac{4L_\alpha^2}{L_\alpha + 4A_\alpha} \quad (3)$$

4) S_α can be approximated by the number of carbides per unit area times the circumference of an average size carbide, assuming they are spherical.

$$S_\alpha = (N_\alpha)\ (\pi\ \bar{L}_\alpha)$$

5) The mean free path (τ) in the two phase alloys,

$$\tau = \left(\frac{4V_\alpha}{S_\alpha} \right) = \frac{4V_\alpha}{N_\alpha \pi \bar{L}_\alpha}$$

REFERENCES

1. Rhines, F. N., "Geometry of Microstructure - Part I and II." Metals Progress, August, 1977, 112, No. 3, pp 60-65 and September, 1977, 112, No. 4, pp 47-51.

2. Moore, G. A., "Is Quantitative Metallography Quantitative?" Applications of Modern Metallographic Techniques, ASTM STP 480, American Society for Testing Materials, 1970, pp. 3-48.

3. Nazare, S. and G. Ondracek. "Automatic Image Analysis in Materials Science." Microscope, 1974, 22, pp. 39-58.

4. Underwood, E. E., "Stereology in Automatic Image Analysis." Microscope, 1974, 22, pp. 70-88.

5. DeHoff, R. T. and F. N. Rhines, Quantitative Microscopy, McGraw-Hill, Inc. 1968.

6. Muscara, J., "A Metallurgical Study of High Stress Abrasion," Doctoral Dissertation, University of Michigan, October, 1971.

DISTRIBUTION LIST

Mr. John J. Mahoney
Senior Contract Administrator
Contracts Management Office
DOE - Chicago Operations Office
9700 South Cass Avenue
Argonne, IL 60439
- 6 copies -

Dr. Thomas Cox
DOE - Fossil Energy Research
Room 4203
20 Massachusetts Avenue
Washington, D.C. 20545

Dr. Paul Scott
DOE - Fossil Energy Research
20 Massachusetts Avenue
Washington, D.C. 20545

Dr. Sam Schnedier
National Bureau of Standards
Washington, D.C. 20234

Dr. John Dodd
Climax Molybdenum Company
13949 West Colfax Avenue
Golden, CO 80401

Metals and Ceramics Information Center
Battelle-Columbus Laboratories
505 King Avenue
Columbus, OH 43201

Dr. J. L. Parks
Climax Molybdenum Research Lab.
1600 Huron Parkway
Ann Arbor, MI 48106

Dr. M. S. Bhat
Materials and Molecular Research
Bldg. 62 - Room 239
Lawrence Berkeley Laboratory
University of California
Berkeley, CA 94720

Mr. Howard Avery
69 Alcott
Mahwah, N.J. 07430

Dr. Kenneth Anthony
Stellite Division
Cabot Corporation
Kokomo, IN 46901

Dr. Stanley Wolf
Materials Science Program
Division of Basic Energy Sciences
DOE
Washington, D.C. 20545